Polyolefin - Graphene Oxide Nanocomposites: Interfacial Interactions and Low Temperature Brittleness Reduction

Vikas Mittal,*[1] *Gisha E. Luckachan*,[1] *Nadejda B. Matsko*[2]

Summary: The interfacial interactions and low temperature brittleness of high density polyethylene (PE)-chlorinated polyethylene (CPE) blends as well as their nanocomposites with graphene oxide (G) were characterized. The filler and the CPE phases were observed to have chemical interaction during solution mixing which enhanced during melt mixing of CPE-graphene oxide masterbatch with PE matrix. Majority of the Cl atoms in the CPE chains were observed to be depleted during chemical reaction or thermal degradation at melt compounding temperature, thus, resulting in chlorine free materials. The samples with CPE35 could not be sufficiently hardened even at −180 °C and remained too soft for cryo-sectioning. The composites had even higher degree of surface roughness due to additional effect of weak filler matrix interactions.

Keywords: chlorinated polyethylene; fillers; graphene oxide; height corrugation; nanocomposite

Introduction

Polyolefins e.g. high density polyethylene (PE) have a wide range of properties like low cost, ease of recycling, good processability, non-toxicity, bio-compatibility, and good solvent resistance.[1,2] It is generally desirable to further expand the range of their service temperatures in order to enhance the spectrum of applications. Chlorinated polyethylene (CPE) is commonly blended with polymers for different purposes such as to improve the toughening properties of matrix polymers,[3] as a compatiblization agent between two polymers,[4,5] to improve processing properties,[6] to tune adhesion properties,[7] to enhance ignition resistance[8] and to modify gas transport properties,[9] however, its use in inducing low temperature flexibility in the polyolefin matrices has not been explored.

Graphene, which consists of one atomic thick sheets of covalently sp^2-bonded carbon atoms in a hexagonal arrangement, has been incorporated in various polymer matrices to enhance electrical and mechanical properties.[10–13] To enhance the compatibility of graphene (and graphene oxide) in various polymer matrices, amphiphilic compatibilizer having polar and non-polar groups are used which result in improved filler dispersion.[14,15] CPE has also been observed to be efficient compatibilizer in composites,[16,17] with extent of filler dispersion proportional to the amount of CPE as well level of chlorination.

Due to the immense potential of graphene in enhancing the material characteristics, further analysis of its nanocomposites with commercially important polymers is required in terms of physical and chemical interactions between the compatibilizer and filler in comparison to interactions between polymer and compatibilizer phases as well as polymer and filler phases. Additional goal of the current study was to study the low temperature brittleness of these blends as well as nanocomposites.

[1] Department of Chemical Engineering, The Petroleum Institute, Abu Dhabi, UAE
E-mail: vmittal@pi.ac.ae
[2] Graz Centre for Electron Microscopy, Graz, Austria

Experimental Part

Materials

Polyethylene (high density) grade BB2581 was provided by Abu Dhabi Polymers Company Limited (Borouge), UAE. Chlorinated polyethylene grades Weipren® 6025 (25% chlorine content, named as CPE25) and CPE 135A (35% chorine content, named as CPE35) were supplied by Lianda Corporation, USA and Weifang Xuran Chemicals, China respectively. Graphene oxide was produced by thermal exfoliation of precursor graphite oxide using modified Hummer's method as reported earlier.[17,18]

Generation of Blends and Nanocomposites

To generate blend samples, polyethylene was melt mixed with CPE25 and CPE35 polymers in mini twin conical screw extruder (MiniLab HAAKE Rheomex CTW5, Germany) using a mixing temperature of 170 °C for three minutes at 60 rpm (batch size of 5 g). Pure polymer was also similarly melt processed at 170 °C. To achieve nanocomposites, CPE was dissolved in *p*-xylene (3% solid content) at 100 °C under reflux and was mixed with sonicated graphene oxide suspension in *p*-xylene at 100 °C.[17] The mixture was cooled to room temperature and was kept overnight at ambient conditions followed by 40 °C for 24 h. The generated CPE-graphene oxide masterbatches were melt mixed with polyethylene at 190 °C using mini twin screw extruder using the similar processing conditions used to form blends. The amount of graphene oxide in the nanocomposites was fixed at 0.5 wt%.

Characterization Methods

AFM images were collected in tapping mode using silicon nitride cantilevers with natural frequencies in the 300 kHz range (force constant 20 N/m, tip radius 10 nm (NT-MDT, Russia)). AFM image processing was performed using Nanoscope v720 software (Veeco, USA).

Rheological data was obtained from AR 2000 rheometer from TA Instruments. Injection molded disc shaped samples with 25 mm diameter and 2 mm thickness were measured at 185 °C using a gap opening of 1.2 mm. Initially, the strain sweep scans were recorded for the samples at $\omega = 1$ rad/s from 0.1 to 100% strain. As the samples were observed to be shear stable up to 10% strain, a strain of 4% was chosen to generate frequency sweep scans of all the samples from $\omega = 0.1$ to 100 rad/s.

IR spectra were collected on Nicolet iS10 spectrometer equipped with SmartiTR diamond ATR accessory (angle of incidence of 45°), DTGS KBr detector and KBr beam splitter. It had a diamond ATR crystal (index of refraction 2.4 at 1000 cm^{-1}) and a depth penetration of 2 μm at 1000 cm^{-1} for sample with refractive index of 1.5. Spectra were recorded by the OMNIC software in the 4000–525 cm^{-1} region with a resolution of 4 cm^{-1} from 16 scans. LINSEIS STA PT1600 simultaneous thermogravimetric analysis - differential thermal analysis (TGA-DTA) system was used to measure the weight change during heating. This system is coupled with a Phipher mass spectrometer (MS) which allowed to determine HCl ($m/z = 36$), H_2O ($m/z = 18$) and CO_2 ($m/z = 44$) elimination during heating. All measurements are realized with a heating rate of 10 °C/min, under air atmosphere (flow rate 20 ml/min).

Tensile testing of composites was performed on universal testing machine (Testometric, UK). The sample dimensions for tensile test were: sample length 73 mm, gauge length 30 mm, width 4 mm and thickness 2 mm. A loading rate of 4 mm/min was used and the tests were carried out at room temperature. Tensile modulus and yield stress were calculated using built in software Win Test Analysis.

Results and Discussion

An earlier study reported the calorimetric properties of the chlorinated polyethylene samples used in the current work.[17] CPE25 was semi-crystalline in nature with a peak melting point of 130 °C, whereas CPE35

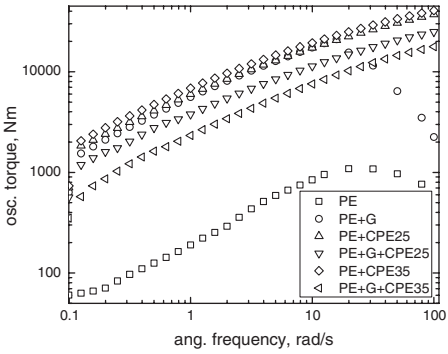

Figure 1.
Oscillatory torque as a function of angular frequency.

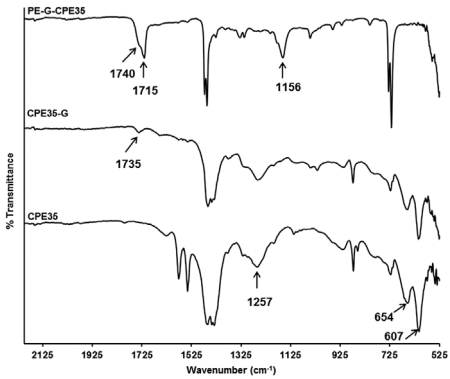

Figure 2.
IR spectra of CPE35, CPE + G and PE + G + CPE35.

was amorphous. Figure 1 shows the oscillatory torque as a function of angular frequency during the rheological testing. The build-up of torque for PE + G, PE + CPE25 and PE + CPE35 followed a similar trend and was higher than the PE, PE + G + CPE25 and PE + G + CPE35 samples. Thus, stiff CPE chains acted as filler particles in the matrix, however, it should also be noted that the amount of graphene in the PE + G composites was very low as compared to CPE amounts in PE + CPE blends. The observed torque was much lower in PE + G + CPE nanocomposites and the least values were obtained for PE + G + CPE35 composite. As graphene oxide has a polar surface, therefore, it is expected to interact positively with CPE chains. CPE35 due to its higher chlorination content can have even enhanced extent of these interactions. As a result, the dispersion of graphene oxide platelets under shear in the PE matrix would improve as extent of polarity of compatibilizer was increased, leading to lower torque generation due to the well dispersed graphene oxide platelets.

Interactions between CPE35 compatibilizer and graphene oxide in PE + G + CPE35 nanocomposite were also studied by IR as shown in Figure 2. In addition to the characteristic C-Cl vibrations of CPE35 at 654 cm^{-1} and 607 cm^{-1}, IR spectrum of CPE35 + G showed a new peak at 1735 cm^{-1} which was attributed to C=O vibrations of ester linkages. This new peak along with the reduced intensity of C—Cl vibrations indicated that C-Cl groups on CPE were involved in a chemical reaction with polar functional groups on graphene oxide (—COOH, —OH) under the mild mixing conditions (100 °C, 30 min sonication). Melt mixing of this composite with PE at 170 °C under shear (60rpm) facilitated more reaction between CPE and graphene oxide, that resulting in an intense C=O vibration peak of ester linkages at 1715 cm^{-1} with a shoulder at 1740 cm^{-1} and C—O vibration peak of ester and ether linkages at 1156 cm^{-1} (Figure 2). Utilization of chlorine for the chemical bonding (ester, ether etc.) between CPE and graphene oxide in PE + G + CPE35 nanocomposite could be further confirmed from the absence of C—Cl vibrations at 654 cm^{-1} and 607 cm^{-1}. CPE25 exhibited exactly similar behavior to that of CPE35 in its composite with graphene oxide and PE, however, the extent of reaction between the functional groups on graphene oxide and CPE25 was less due to the low percentage of chlorine content that could be observed in the IR spectrum of PE + G + CPE25 as a low intense C=O vibration at 1737 cm^{-1}. Interestingly, IR spectra of PE + CPE35 and PE + CPE25 didn't show any features from CPE part which indicated that C—Cl bonds would have been destroyed at higher temperature used during compounding.

DTA plot of CPE35 given in Figure 3 showed three endothermic peaks

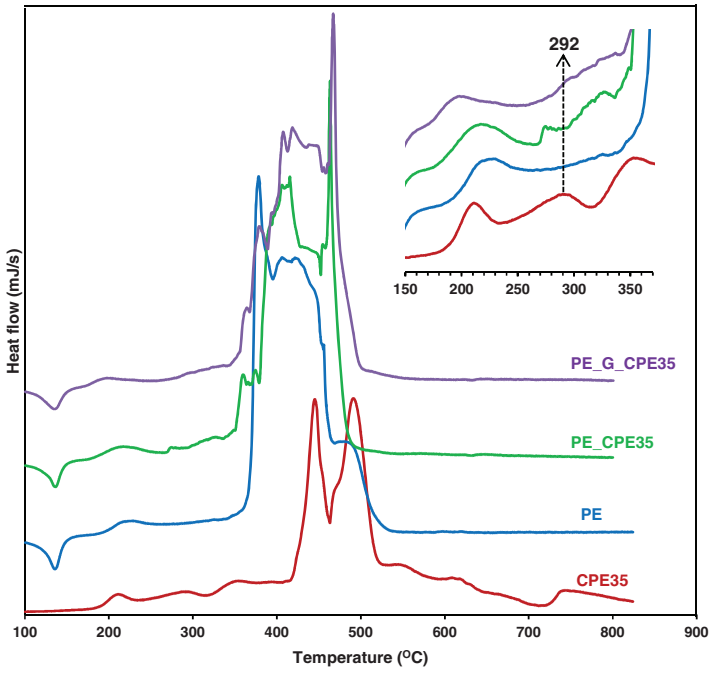

Figure 3.
DTA plots of PE, CPE35, PE + CPE35 and PE + G + CPE35.

corresponding to the first thermal degradation step in TGA (150 °C–360 °C). Melting phenomena seemed to result in loss of water and some amorphous carbon as it showed small humps at 211 °C in the mass spectrometer profiles of H_2O (m/z = 18) and CO_2 (m/z = 44). The second endothermic peak (T_{max} = 292 °C) in the DTA plot of CPE35 could be assigned to the loss of chlorine because the mass spectra contains HCl (m/z = 36) profile in the temperature range of 250 °C to 350 °C. CPE35-G exhibited similar thermal behavior as pure CPE.

Comparison of DTA plot of CPE35 with those of PE as well as PE-CPE35 revealed that all plots had first endothermic peak, but for PE, the second endothermic peak was absent (Figure 3). It thus confirmed that the second endothermic peak in the DTA plot of PE + CPE35 was from the loss of HCl which appeared as small but clearly visible contribution at 273 °C (T_{max}). Even though the amount of CPE in PE + CPE35 was only 5wt%, the evolution of HCl was clearly detected in the DTA plot. The final composite PE + G + CPE35 showed a significant decrease in the intensity of second endothermic peak and/or it appeared as a small shoulder around 300 °C. Thus, it could be concluded that the amount of chlorine in PE + CPE35 and PE + G + CPE35 decreased significantly due to the destruction of C-Cl bond during melt compounding. The amount of remaining Cl in the PE + G + CPE35 was even lower than the PE + CPE35 blend due to significant depletion of Cl atoms during their reactions with functional groups on graphene oxide which resulted in strong chemical bonds such as ester, ether etc. between CPE chains and graphene oxide as confirmed from FTIR. Similar findings were also observed for CPE25 system. Thus, though the addition of CPE phase was required to achieve interfacial interactions, the final product did not contain significant content of Cl, thus, still retaining the commercial attractiveness of the generated nanomaterials.

Figure 4 shows the relative tensile modulus of the samples in comparison to pure polyethylene.[17] The pure polymer had a tensile modulus of 1063 MPa. The modulus of PE + G nanocomposite was improved by 7% as compared to pure polymer. Addition of 5% CPE35 reduced the modulus to 75% of the pure polymer due to matrix plasticization, however, the nanocomposite modulus was 85% of pure polymer. Addition of 10% CPE35 to PE further reduced the modulus, but the nanocomposite exhibited a marginal increase in the modulus due to dominant contribution of filler exfoliation and resulting stress transfer as compared to negative impact of phase immiscibility and matrix plasticization. Thus, the overall enhancement in the tensile modulus was a result of competing factors related to system components, interfacial interactions and material morphology. The matrix plasticization due to the addition of compatibilizer resulted in its decrease, whereas the enhanced filler exfoliation due to better interfacial interactions enhanced it. In terms of achieving the materials with low temperature flexibility, graphene nanocomposites with 5% and 10% CPE35 content were optimum as the mechanical performance of the pure polymer was retained. Also, the addition of graphene platelets did not negatively impact the reduced low temperature brittleness of the nanocomposites.

Surface topography analysis was performed at three different places on the block surface block faces prepared by microtoming at −140 °C and corresponding topography variation was analyzed. It is noteworthy that all parameters related to hardness of conventional PE such as the elastic constants, tensile strength and crushing strength increased with decreasing temperature, indicating that the cryosectioning of polycrystalline PE became more difficult at lower temperature. Incorporation of the amorphous CPE35 to PE, however, resulted in completely different behavior. Figure 5 demonstrates the quantitative analysis of the surface topography of the samples. The values represent an average of three measurements of height corrugation at different places of the scanned area shown in the micrographs (25 μm^2). The height variation enhanced on adding CPE to polyethylene indicating the plasticization of the matrix on the addition of low molecular weight polymer. The extent of plasticization was higher in the case of amorphous CPE35 polymer where the height variation was significantly large as compared to PE blend with CPE25.

The composites followed similar trend as the polymer blends, however, the height variation was even higher in the composite samples (Figure 6). For example, for PE + G sample, a value of 113 nm for surface variation was calculated which was enhanced markedly to 198 nm for

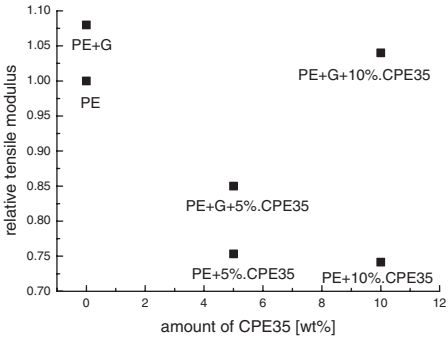

Figure 4.
Relative tensile modulus of polymer blends and nanocomposites in comparison with pure polymer.

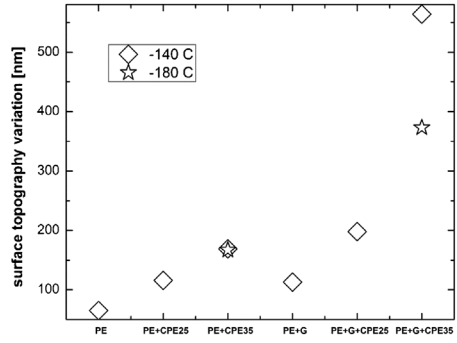

Figure 5.
Surface topography variation of blends and nanocomposites at −140 °C and −180 °C.

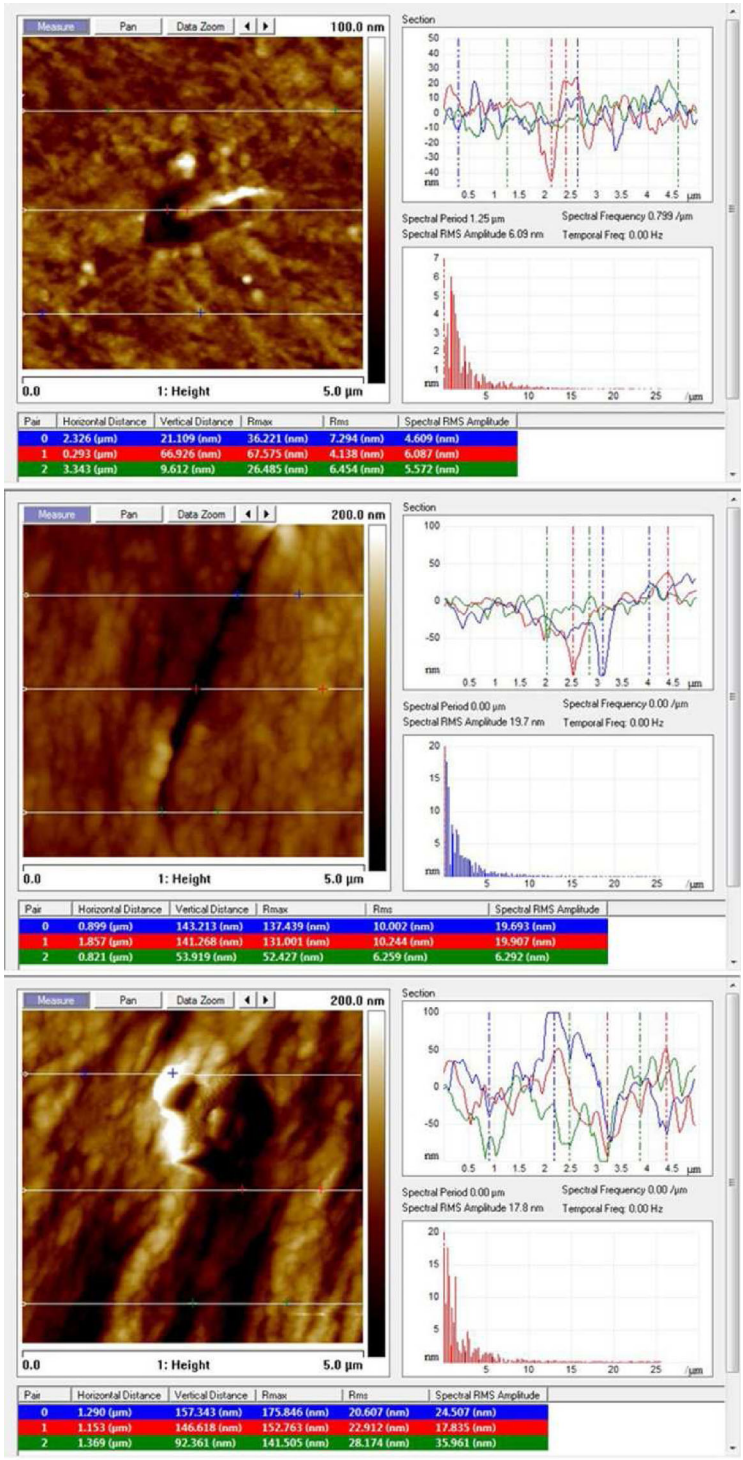

Figure 6.
AFM height images and corresponding height corrugation analysis for PE + G (top image), PE + G + 5%CPE25 (middle row) and PE + G + 5%CPE35 (bottom row) when sectioned at −140 °C.

PE + G + CPE25 and 564 nm for PE + G + CPE35 nanocomposites. It indicated that the addition of small amount of graphene oxide did not negatively impact the flexibility of the samples. Much higher values of height corrugation also indicated towards weak interfacial connections between the polymer and filler phases. It should also be noted that though the CPE polymer is expected to have better interfacial interaction with the filler surface due to compatibility with the hydroxyl, epoxy or carboxyl groups present on graphene oxide surface, but it may have also induced phase immiscibility in nanocomposites due to its higher concentration near the graphene oxide surface. The extent of immiscibility would thus increase as more polar polymer (e.g. CPE35) is added to the polyethylene matrix. As a result, this would also lead to observed higher height variation as a function of CPE polarity. Figure 5 also shows the analysis of the block faces of PE + CPE35 and PE + G + CPE35 samples when the sectioning was performed at −180 °C. All other samples exhibited a brittle fracture. The sectioning in the case of compounds containing CPE35 indicated that the system was still rather soft and flexible, though reduced values of height corrugation were observed as compared to the case at −140 °C.

Conclusion

IR confirmed a chemical reaction between the CPE and graphene oxide platelets. The blends of PE and CPE did not show C-Cl peaks thus indicating that the Cl was depleted not only due to the chemical reaction, but also by thermal degradation, which was also confirmed by DTA-MS analysis. The hardness/flexibility could be qualified using the height variation in the AFM height images. The height variation was more pronounced in the case of nanocomposites indicating that the filler could be pulled out during sectioning. The blend and composite samples with CPE35 content could both be sectioned at −140 °C and −180 °C without brittle fracture, thus, confirming the flexibility at lower temperature. It was also observed that graphene oxide addition enhanced the mechanical performance of the composites and had dominant effect as compared to the plasticization effect induced by CPE addition.

[1] J. Jancar, "*Mineral Fillers in Thermoplastics I: Raw Materials and Processing*", Springer-Verlag, Berlin **1999**.
[2] U. Hippi, "*Polyolefin Composites*", John Wiley & Sons, New Jersey **2008**.
[3] L. Zhou, X. Wang, Y. Lin, J. Yang, Q. Wu, *J. Appl. Polym. Sci.* **2003**, *90*, 916.
[4] E. A. Eastwood, M. D. Dadmun, *Polymer* **2002**, *43*, 6707.
[5] P. He, H. Huang, W. Xiao, S. Huang, S. Cheng, *J. Appl. Polym. Sci.* **1997**, *64*, 2535.
[6] S. Stoeva, *J. Appl. Polym. Sci.* **2006**, *101*, 2602.
[7] S. Waddington, D. Briggs, *Polym. Commun.* **1991**, *32*, 506.
[8] US-5525651 (**1996**), inv.S. A. Ogoe.
[9] J. A. Barrie, W. D. Webb, *Polymer* **1989**, *30*, 327.
[10] P. Mukhopadhyay, R. K. Gupta, *Plast. Eng.* **2011**, 32.
[11] H. Kim, A. A. Abdala, C. W. Macosko, *Macromolecules* **2010**, *43*, 6515.
[12] M. A. Rafiee, J. Rafiee, Z. Wang, H. Song, Z. Z. Yu, N. Koratkar, *ACS Nano* **2009**, *3*, 3884.
[13] D. A. Nguyen, Y. R. Lee, A. V. Raghu, H. M. Jeong, C. M. Shin, B. K. Kim, *Polym. Int.* **2009**, *58*, 412.
[14] H. C. Schniepp, J.-L. Li, M. J. McAllister, H. Sai, M. Herrera-Alonso, D. H. Adamson, R. K. Prud'homme, R. Car, D. A. Saville, I. A. Aksay, *J. Phys. Chem. B* **2006**, *110*, 8535.
[15] S. Sanchez-Valdes, M. L. Lopez-Quintanilla, *Adv. Sci. Technol.* **2006**, *45*, 1399.
[16] V. O. Guffey, A. B. Sabbagh, *J. Vinyl Addit. Technol.* **2002**, *8*, 259.
[17] A. U. Chaudhry, V. Mittal, *Polym. Eng. Sci.* **2013**, *53*, 78.
[18] M. J. McAllister, J. L. Li, D. H. Adamson, H. C. Schniepp, A. A. Abdala, J. Liu, M. Herrera-Alonso, D. L. Milius, R. Car, R. K. Prud'homme, I. A. Aksay, *Chem. Mater.* **2007**, *19*, 4396.

